

Realization of tunable spin-dependent splitting in intrinsic photonic spin Hall effect

Xiaohui Ling,^{1,2,3} Xunong Yi,¹ Xinxing Zhou,² Yachao Liu,² Weixing Shu,² Hailu Luo,^{1,2, a)} and Shuangchun Wen²

¹*SZU-NUS Collaborative Innovation Center for Optoelectronic Science and Technology, and Key Laboratory of Optoelectronic Devices and Systems of Ministry of Education and Guangdong Province, College of Optoelectronic Engineering, Shenzhen University, Shenzhen 518060, China*

²*Laboratory for spin photonics, College of Physics and Microelectronic Science, Hunan University, Changsha 410082, China*

³*Department of Physics and Electronic Information Science, Hengyang Normal University, Hengyang 421002, China*

(Dated: 6 October 2018)

We report the realization of tunable spin-dependent splitting in intrinsic photonic spin Hall effect. By breaking the rotational symmetry of a cylindrical vector beam, the intrinsic vortex phases that the two spin components of the vector beam carries, which is similar to the geometric Pancharatnam-Berry phase, is no longer continuous in the azimuthal direction, and leads to observation of spin accumulation at the opposite edge of the beam. Due to the inherent nature of the phase and independency of light-matter interaction, the observed photonic spin Hall effect is intrinsic. Modulating the topological charge of the vector beam, the spin-dependent splitting can be enhanced and the direction of spin accumulation is switchable. Our findings may provide a possible route for generation and manipulation of spin-polarized photons, and enables spin-based photonics applications.

Photonic spin Hall effect (SHE) describes the mutual influence of the photon spin (polarization) and the trajectory (orbit angular momentum) of light beam propagation, i.e., spin-orbit interaction¹⁻³. It manifests as spin-dependent splitting (SDS) of light, which corresponds to two types of geometric phases: the Rytov-Vladimirskii-Berry phase associated with the evolution of the propagation direction of light and the Pancharatnam-Berry phase related to the manipulation with the polarization state of light³⁻⁵. When a light beam reflecting/refracting at a planar interface or passing through an inhomogeneous anisotropic medium, it may acquire a locally varying geometric phase, i.e., the different part of the beam carrying different geometric phase⁵⁻⁹. The interference upon transmission leads to the redistribution of the beam intensity and may show a SDS of light, that is, the photonic SHE. Recent advances in this field provide new opportunities for advantageous measurement of the optical parameters of nanostructures such as metallic film and graphene^{10,11}. More importantly, it offers a possible way for generation and manipulation of spin-polarized photons and spin/orbital angular momenta of light, and enables spin-controlled photonics applications^{12,13}.

At the interface reflection and refraction of different media, the SDS induced by the photonic SHE is generally very tiny and sensitive to the optical parameters of the media (e.g., refractive indices and thickness, etc.) which makes it difficult to manipulate the SDS with a real medium interface^{5,6,14}. An inhomogeneous anisotropic medium can produce a giant and tunable SDS in momentum space¹⁵⁻¹⁷, but it requires a complex and precise fabrication technique to construct the medium. Actually, the photonic SHE does not always rely on the light-matter interaction; it can be observed in an oblique observation plane respect to the beam propagation direction

even in the free space^{18,19}. This effect is intrinsically dependent upon the polarization geometry of the beam projected on the oblique observation plane rather than any kind of light-matter interaction. Similar to the photonic SHE occurring at the interface reflection and refraction, the induced SDS is fixed and also exceedingly weak.

In this work, we report the realization of tunable SDS in intrinsic photonic SHE by blocking part of a cylindrical vector beam (CVB) with a fan-shaped aperture (FSA). The underlying mechanism is attributed to the inherent, opposite vortex phase that the two spin components (circular polarizations) of the CVB carry, so the observed photonic SHE is intrinsic. This phase is similar to the geometric Pancharatnam-Berry phase which creates a geometric phase gradient in momentum space, and results in the SDS²⁰. By modulating the topological charge of the CVB, the SDS can be enhanced, and the direction of spin accumulation is switchable.

The CVB that exhibits inhomogeneous polarization distribution with rotational symmetry has drawn great attention due to its great potential in many fields including optical manipulation, nonlinear optics, and optical communications (see²¹ for a review and the references therein). It can be viewed as superposition of two sub-beams carrying opposite spin angular momentum (circular polarization) and opposite orbital angular momentum (vortex phase), and can be geometrically represented by the so-called higher order Poincaré sphere^{22,23}. The algebraical description is represented by the following equation:

$$|\psi\rangle = \cos\left(\frac{\phi}{2}\right)|R\rangle e^{-i\beta} + \sin\left(\frac{\phi}{2}\right)|L\rangle e^{i\beta}. \quad (1)$$

Here, ϕ is a tuning parameter. $|R\rangle e^{i\beta}$ and $|L\rangle e^{-i\beta}$ are circularly polarized vortex light, with $|R\rangle$ and $|L\rangle$ standing for the right- and left-circular polarizations, respectively. For $\phi = \pi/2$, Eq. (1) indicates a linear polarized CVB. In this case, the Jones vector of the CVB can be simply written as

^{a)}Electronic mail: hailuluo@hnu.edu.cn

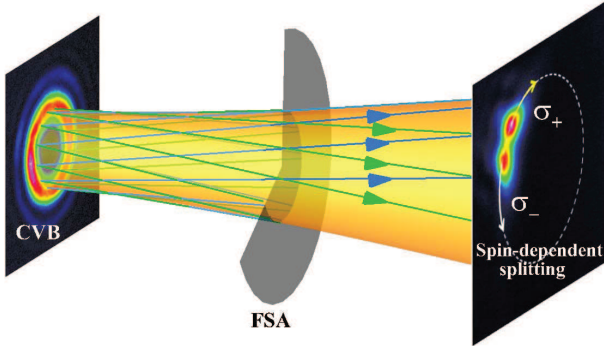


FIG. 1. Schematic illustration of the intrinsic photonic SHE of the CVB. The blue and green rays with arrows indicate the local wave vectors of the two spin components of the CVB. The rotational symmetry is broken by blocking part of the CVB with a FSA. It shows a direct intensity splitting of the left- and right-handed circular polarization components (σ_+ and σ_-).

$(\cos\beta, \sin\beta)^T$ where $\beta = m\varphi + \beta_0$ with m the topological charge, φ the azimuthal angle, and β_0 a constant. Other values of ϕ represent elliptical polarized CVB. Equation (1) unambiguously illustrates that the two circular polarizations carry just opposite azimuthal vortex phase $e^{\pm i\beta}$. This phase is similar to the geometric Pancharatnam-Berry phase which can be obtained in some inhomogeneous anisotropic media^{7,8,16,24,25}. Although the two components have opposite vortex phases and local energy flows, their superposition does not show a helical wave front. They always superpose exactly at the same position and no SDS can be observed, due to the rotational symmetry. When blocking part of a vortex, its intensity distribution and the geometric shadow area just behind the obstacle rotate in the sense of the vortex's handedness^{26,27}, so the two spin components of the CVB no longer superpose exactly and separate from each other (see the schematic picture in Fig. 1).

To measure the intrinsic photonic SHE, we set up a Sagnac interferometer to generate the linear polarized CVB, as shown in Fig. 2(a), which can also be conveniently generated by many other methods^{21,28-30}. This apparatus relies on the superposition of two equal-intensity beams with opposite circular polarizations and opposite vortex phases, according to Eq. (1). The polarizer (P1) can ensure the light output from the He-Ne laser to be 45° polarization respect to the horizontal direction. Then the beam passes through the polarization beam splitter (PBS) and is split into two equal-intensity beams with the transmission beam being horizontal polarization and the reflection beam vertical polarization. The two sub-beams propagate exactly in a common path. A phase-only spatial light modulator (SLM) is used at small incidence angle, and can apply a vortex phase with any desired topological charge to a horizontal polarization beam which is a good approximation of phase vortex-bearing Laguerre-Gauss beam. A half-wave plate (HWP1) with its optical axis 45° inclined to the horizontal direction is employed to change the vertical polarization to a horizontal one and vice versa for its counter-propagating counterpart. A Dove prism (DP) involves one reflection to change the sign of the topological charge alone

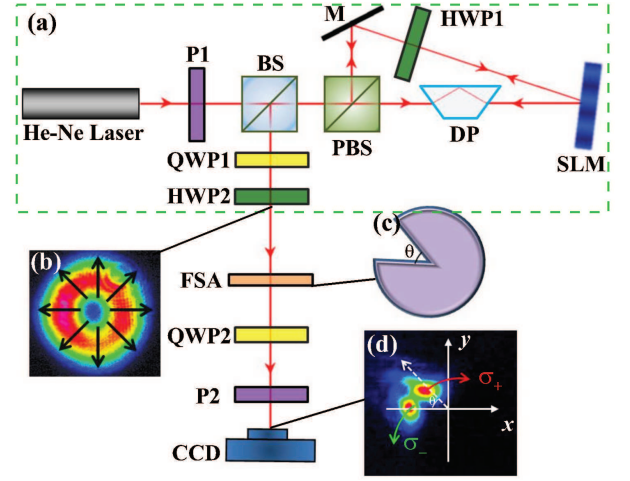


FIG. 2. Experimental setup for generating the CVB and measuring the photonic SHE when it passing through a fan-shaped aperture (FSA). (a) The laser source is a single mode linearly polarized He-Ne laser, wavelength $\lambda = 632.8$ nm. The polarizer (P1) ensures a 45° polarization light to impinge into the polarization beam splitter (PBS) and being equally split into two sub-beams. The Sagnac interferometer comprised of a PBS, a phase-only spatial light modulator (SLM, Holoeye Pluto-Vis, Germany), a Dove prism (DP), a half-wave plate (HWP1) and a mirror (M). A quarter-wave plate (QWP1) changes the two sub-beams from linear polarization to opposite circular polarizations. Then a CVB is produced after the QWP1. Another half-wave plate (HWP2) is used to modulate the polarization distribution of the CVB. BS represents a non-polarizing beam splitter. (b) An example of the generated CVB with radial polarization distribution. (c) Schematic picture of the FSA. (d) CCD recorded intensity of the CVB passing through the FSA without the Stokes parameter measurement setup (QWP2 and P2). It shows a direct intensity splitting of the σ_+ and σ_- components.

one beam path, and ensures that the output beam contains two opposite phase vortices. Then we use a quarter-wave plate (QWP1) with 45° optical axis orientation changes the two sub-beams into opposite circular polarizations. So the CVB is generated after the QWP1 [see Fig. 2(b)] and its intensity shows a donut-shaped profile similar to a vortex beam. The HWP2 can help to modulate the polarization distribution of the CVB, e.g., changing a radial polarization into an azimuthal polarization or any intermediate states²⁰.

The generated CVB then passes through a FSA [Fig. 2(c)] at normal incidence. For the sake of simplicity and without loss of generality, the FSA can be described by the following expression:

$$T(\theta) = \begin{cases} 1 & \text{for } \theta \text{ radian} \\ 0 & \text{otherwise.} \end{cases} \quad (2)$$

It is known that the Stokes parameter S_3 can be used to describe the circular polarization degree³¹, so the SDS of light can be obtained by measuring the S_3 parameter pixel by pixel in the output using a typical setup: a quarter-wave plate (QWP2), a polarizer (P2), and a CCD camera. In the

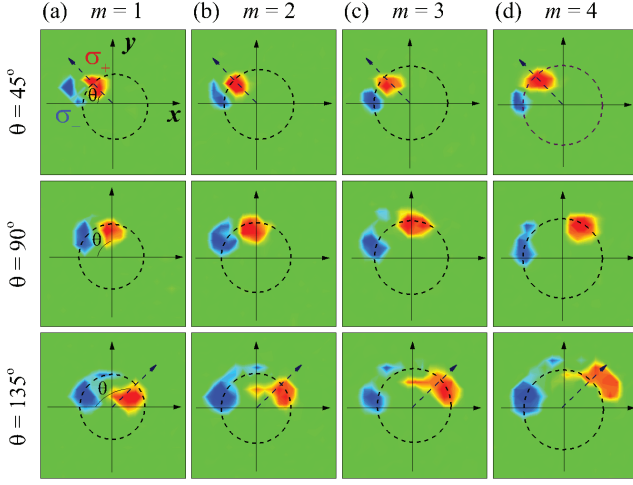


FIG. 3. Intrinsic photonic SHE of the CVB with different topological charges for different FSAs with three typical aperture angles θ . The dashed circles indicate the profile of the incident CVB. The experimentally measured light spot of the S_3 parameters have a little deviation from the dashed circles because of the unavoidable experimental errors in the process of the S_3 measurement.

experiments, the S_3 parameter can be given by

$$S_3 = \frac{I_{\sigma+} - I_{\sigma-}}{I_{\sigma+} + I_{\sigma-}}. \quad (3)$$

Here, $I_{\sigma+}$ and $I_{\sigma-}$ represent the intensities measured in the circular polarization basis, respectively.

We first consider the influence of the topological charge m on the intrinsic photonic SHE. The vortex phase creates a phase gradient in the azimuthal direction, which results in a SDS in k (momentum) space: $\Delta k = \sigma_{\pm} \nabla \beta = \sigma_{\pm} m \hat{e}_{\varphi}$ with $\sigma_{\pm} = \pm 1$ representing the left and right circular polarization and \hat{e}_{φ} the unit vector in the azimuthal direction, respectively^{12,20}. Hence, this shift is proportional to the value of m . However, for a CVB, the SDS cannot be observed in free-space propagation, due to its rotational symmetry. Breaking the rotational symmetry, it is expected to observe the spin accumulation at the edge of the beam.

Figure 3 shows the measured S_3 parameters of the photonic SHE for different CVBs and different aperture angles θ . The spin-dependent shift increases with the rise of the value of m . On the other hand, the shift distance is limited by the dimension of the aperture angle because the spin-polarized photons

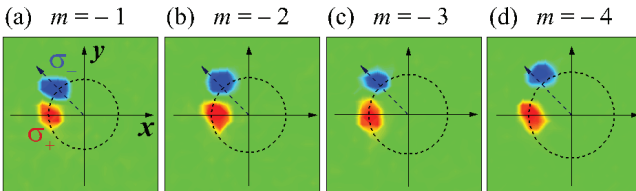


FIG. 4. Intrinsic photonic SHE of the CVB with negative topological charges $m = -1, -2, -3$, and -4 for the aperture angle of the FSA $\theta = 45^\circ$.

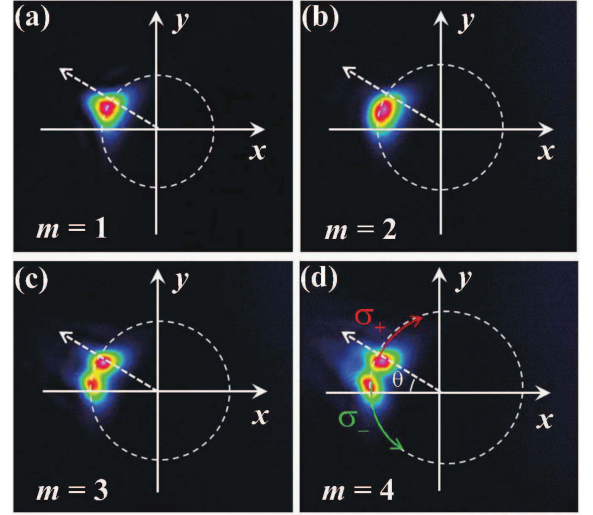


FIG. 5. Direct intensity illustration of the giant photonic SHE with the aperture angle of the FSA $\theta = 30^\circ$. The four experimental screen-shots show the results of CVBs with different topological charges m .

accumulate at the beam edge. Also because of this, the spin-dependent splitting increases with the increase of θ . If reversing the sign of m by modulating the phase picture displayed on the SLM, the direction of spin accumulation is also inverted, as shown in Fig. 4. Because the sign of m directly determines the handedness of the vortex phase that the two spin components of the CVB carry. The measured S_3 parameters have a little deviation from the expected position (dashed circles in Figs. 3 and 4) due to the unavoidable experiment errors in the S_3 measurement.

The SDS of the intrinsic photonic SHE of the CVB can be large enough for direct measurement without using the weak measurement technology^{5,32}. With the increase of the value m of the CVB, we can directly observe the intensity separation of the σ_+ and σ_- components, as shown in Fig. 5 for $\theta = 30^\circ$. In (a) and (b) for $m = 1$ and 2 , the two components do not separate enough from each other and show a single-spot profile, however, it still can be discriminated by measuring the S_3 parameter just like in Figs. 3 and 4. If the phase gradient is large enough, the σ_+ and σ_- components are almost completely separated, as shown in Fig. 5(c) and 5(d). The induced spin-dependent shift is within millimeters (the beam waist of the He-Ne laser is 0.7 mm and expanded to 2.1 mm by a beam expander), which is many times larger than the optical wavelength (632.8 nm). It is also much larger than that had observed previously in beam reflection and refraction with the shift of the order of a fraction of wavelength^{5,6,13}. This enables us to observe a giant photonic SHE.

Actually, the focusing behavior of the CVB with axial symmetry broken by a lens has been explored, and its application in optical trapping was suggested³³. In the focal plane, the circular polarizations have a spin-dependent rotation with their rotation angle reaching to $\pi/2$ relative to the aperture edge²⁶. This is due to that the scalar vortex beam has an azimuthal energy flow along the circumference of the beam

when it propagates³⁴. In our context, we consider the intrinsic SHE of the CVB with rotational symmetry breaking at a propagation distance much less than the Rayleigh distance, so the spin-polarized photons accumulate at the opposite edge of the beam. As mentioned above, the SDS occurs in the k space in the azimuthal direction, the induced shift would increase linearly upon beam propagation. Opposite topological charge just reverses the direction of spin accumulation.

In summary, we have experimentally demonstrated the realization of tunable SDS in intrinsic photonic SHE of the CVB by breaking its rotational symmetry using a FSA to block part of the CVB. The spin accumulation occurs at the edge of the beam, and the SDS increases with the topological charge of the CVB and restricts by the aperture angle of the FSA. The underlying mechanism is attributed to the discontinuous local energy flow that results from the broken, opposite vortex phases. It is large enough to be directly observed without using a weak measurement technology. Because of the inherent nature of the phase and independency of light-matter interaction, the observed photonic SHE is intrinsic. This enables us to observe a direct and giant photonic SHE. Our findings reveal that the photonic SHE may be manipulated (enhanced or inverted) by directly tailoring the polarization geometry of light, which may provide a possible route for generation and manipulation of spin-polarized photons, and enables spin-controlled photonics applications.

This research was supported by the National Natural Science Foundation of China (Grants No. 61025024, No. 11274106, and No. 11347120), the Scientific Research Fund of Hunan Provincial Education Department of China (Grant No. 13B003), and the Doctorial Start-up Fund of Hengyang Normal University (Grant No. 13B42).

¹M. Onoda, S. Murakami, and N. Nagaosa, Phys. Rev. Lett. **93**, 083901 (2004).

²K. Y. Bliokh and Y. P. Bliokh, Phys. Rev. Lett. **96**, 073903 (2006).

³K. Y. Bliokh, A. Niv, V. Kleiner, and E. Hasman, Nat. Photon. **2**, 748 (2008).

⁴K. Y. Bliokh, Y. Gorodetski, V. Kleiner, and E. Hasman, Phys. Rev. Lett. **101**, 030404 (2008).

⁵O. Hosten and P. Kwiat, Science **319**, 787 (2008).

⁶Y. Qin, Y. Li, H. He, and Q. Gong, Opt. Lett. **34**, 2551 (2009).

⁷Z. Bomzon, V. Kleiner, and E. Hasman, Opt. Lett. **26**, 1424 (2001).

⁸L. Marrucci, C. Manzo, and D. Paparo, Phys. Rev. Lett. **96**, 163905 (2006).

⁹J. Ren, Y. Li, Y. Lin, Y. Qin, R. Wu, J. Yang, Y. Xiao, H. Yang, and Q. Gong, Appl. Phys. Lett. **101**, 171103 (2012).

¹⁰X. Zhou, X. Ling, H. Luo, and S. Wen, Appl. Phys. Lett. **101**, 251602 (2012).

¹¹X. Zhou, Z. Xiao, H. Luo, and S. Wen, Phys. Rev. A **85**, 043809 (2012).

¹²N. Shitrit, I. Yulevich, E. Maguid, D. Ozeri, D. Veksler, V. Kleiner, and E. Hasman, Science **340**, 724 (2013).

¹³X. Yin, Z. Ye, J. Rho, Y. Wang, and X. Zhang, Science **339**, 1405 (2013).

¹⁴H. Luo, X. Ling, X. Zhou, W. Shu, S. Wen, and D. Fan, Phys. Rev. A **84**, 033801 (2011).

¹⁵N. Shitrit, I. Bretner, Y. Gorodetski, V. Kleiner, and E. Hasman, Nano Lett. **11**, 2038 (2011).

¹⁶X. Ling, X. Zhou, H. Luo, and S. Wen, Phys. Rev. A **86**, 053824 (2012).

¹⁷G. Li, M. Kang, S. Chen, S. Zhang, E. Y. B. Pun, K. W. Cheah, and J. Li, Nano Lett. **13**, 4148 (2013).

¹⁸A. Aiello, N. Lindlein, C. Marquardt, and G. Leuchs, Phys. Rev. Lett. **103**, 100401 (2009).

¹⁹J. Karger, A. Aiello, V. Chille, P. Banzer, C. Wittmann, N. Lindlein, C. Marquardt, and G. Leuchs, Phys. Rev. Lett. **112**, 113902 (2014).

²⁰X. Ling, X. Zhou, W. Shu, H. Luo, and S. Wen, Sci. Rep. **4**, 5557 (2014).

²¹Q. Zhan, Adv. Opt. Photon. **1**, 1 (2009).

²²A. Holleczek, A. Aiello, C. Gabriel, C. Marquardt, and G. Leuchs, Opt. Express **19**, 9714 (2011).

²³G. Milione, H. I. Sztul, D. A. Nolan, and R. R. Alfano, Phys. Rev. Lett. **107**, 053601 (2011).

²⁴A. Niv, Y. Gorodetski, V. Kleiner, and E. Hasman, Opt. Lett. **33**, 2910 (2008).

²⁵E. Karimi, S. A. Schulz, I. De Leon, H. Qassim, J. Upham and R. W. Boyd, Light: Sci. Appl. **3**, e167 (2014).

²⁶J. A. A. J. J. Mod. Opt. **50**, 1573 (2003).

²⁷J. A. Davis and J. B. Bentley, Opt. Lett. **30**, 3204 (2005).

²⁸Z. Bomzon, G. Biener, V. Kleiner, and E. Hasman, Opt. Lett. **27**, 285 (2002).

²⁹X. L. Wang, J. Ding, W. J. Ni, C. S. Guo, and H. T. Wang, Opt. Lett. **32**, 3549 (2007).

³⁰P. H. Jones, M. Rashid, M. Makita, and O. M. Maragò, Opt. Lett. **34**, 2560 (2009).

³¹M. Born and E. Wolf, *Principles of Optics (7th edition)* (Cambridge University Press, Cambridge, 1999).

³²J. Dressel, M. Malik, F. M. Miatto, A. N. Jordan, and R. W. Boyd, Rev. Mod. Phys. **86**, 307 (2014).

³³X. L. Wang, K. Lou, J. Chen, B. Gu, Y. Li, and H. T. Wang, Phys. Rev. A **83**, 063813 (2011).

³⁴M. J. Padgett and A. Allen, Opt. Commun. **121**, 36 (1995).